STM JOURNALS

Journal of
Polymer & Composites

ISSN: 2321-2810 (Online)
ISSN: 2321-8525 (Print)
Volume 14, Special Issue 2, 2026
DOI (Journal): 10.37591/JoPC

https://journals.stmjournals.com/jopc

Research JoPC

A Computational Study of Lift and Drag Characteristics for NACA 4415 and NACA 2412 Aerofoils

Digambar Tukaram Kashid[1,*], Sandeep Sitaram Wangikar[2]

Abstract

The performance of an aerofoil is crucial in designing wind turbine blades, aircraft wings, and other aerodynamic surfaces. This project presents a comparative analysis of two widely used aerofoil profiles, NACA 4415 and NACA 2412, to study their lift and drag characteristics under different flow regimes. The aerofoil geometries were developed using the NACA four-digit notation and modeled in ANSYS Design Modeler. Numerical simulations were conducted in ANSYS Fluent for Reynolds numbers ranging from 10,000 to 200,000 with angles of attack (AOA) of 0°, 15°, 30°, 45°, and 60°. A C-type computational domain with fine-structured meshing was employed to accurately capture external flow behavior. For both aerofoils, lift force (F_L), drag force (F_D), and their respective coefficients (C_L, C_D) were determined. Results show that lift and drag forces increase with higher Reynolds numbers and AOAs, with peak values typically observed at 30° or 45°, depending on the profile. At Re = 200,000, NACA 4415 achieved a maximum lift of 777.25 N at 30° with a drag of 209.20 N, while NACA 2412 produced a maximum lift of 86.69 N and drag of 82.11 N at 45°. Overall, both aerofoils demonstrate better performance at moderate AOAs, though NACA 4415 exhibits superior lift capability, making it more suitable for applications requiring enhanced lifting performance. This study highlights the influence of geometric differences on aerofoil behavior and provides valuable insights for optimizing aerodynamic systems.

Keywords: NACA 4415, NACA 2412, computational fluid dynamics (CFD), drag coefficient (C_D), lift coefficient (C_L), angle of attack (AoA), reynolds number

INTRODUCTION

By the late 1920s and early 1930s the National Advisory Committee for Aeronautics (NACA) had evolved a formal system of aerofoil Classification to rationalise the design and study of aerofoil shapes. This led to formation of NACA four-digit series with each digit signifying important geometrical parameters of the aerofoil.

Aerofoils may be defined by certain specifications; for example, NACA 2412 denotes a design with a maximum camber of 2%, 40% of the chord length from the leading edge, and 12% of the chord thickness. Similarly, NACA 4415 denotes a 4% camber at 40% chord with 15% thickness. These standardizations simplified the selection process for engineers, enabling them to choose profiles tailored for specific aerodynamic performance requirements.

Among the numerous aerofoils in this series, NACA 2412 and NACA 4415 have gained widespread application due to their balanced aerodynamic performance. NACA 2412, with its moderate camber and thickness, offers efficient lift generation. It is appropriate for general flying even

***Author for Correspondence**
Digambar Tukaram Kashid

[1]Research Scholar, Department of Mechanical Engineering, SVERI's College of Engineering, Pandharpur, Maharashtra, India
[2]Associate Professor, Department of Mechanical Engineering, SVERI's College of Engineering, Pandharpur, Maharashtra, India

Received Date: September 05, 2025
Accepted Date: October 08, 2025
Published Date: April 23, 2026

Citation: Digambar Tukaram Kashid, Sandeep Sitaram Wangikar. A Computational Study of Lift and Drag Characteristics for NACA 4415 and NACA 2412 Aerofoils. Journal of Polymer & Composites. 2026; 14(Special Issue 2): S1298–S1315p.

at low angles of attack unmanned aerial vehicles (UAVs), and wind turbine blade design. Conversely, NACA 4415 with a larger camber to thickness ratio, is more often used in wind turbine blades, because in these applications higher lift and pressure recovery are crucial to the efficiency of energy conversion. Such profiles also occur in automotive engineering and aeronautical engineering applications, where safety is of primary importance, where stability and predictable aerodynamic characteristics are vital to design.

LITERATURE REVIEW

Much of the aerodynamic properties have been examined on the NACA aerofoil series and specifically lift, drag, and flow patterns as a consequence of different regimes.

Studies have demonstrated that mesh configuration significantly influences the simulation accuracy of the NACA 2412 aerofoil. Structured meshes provide superior accuracy in capturing flow characteristics compared to unstructured meshes, which is vital for precise CFD analysis of aerofoils [1]. CFD simulation of transonic turbulent flow over the NACA 0012 aerofoil revealed the importance of resolving pressure distribution near the leading edge, which is crucial for stall prediction and aerofoil design under varying flight regimes [2]. Analysis of the NACA 2412 aerofoil incorporating high-lift devices for UAV applications showed notable improvements in lift generation, supporting its applicability in low-speed flight regimes where efficient lift is paramount [3]. Optimization studies on NACA airfoils for sustainable medical delivery UAVs have highlighted that appropriate aerofoil selection and configuration can significantly enhance aerodynamic efficiency and flight endurance [4].

CFD simulations of a sports car model fitted with a rear spoiler shaped as a NACA 2412 aerofoil showed significant increases in downforce at various speeds (100 km/h, 180 km/h, and 240 km/h), thereby improving vehicle stability and control, although accompanied by an increase in drag [5]. CFD investigations of the NACA 0018 aerofoil examined the influence of angle of attack on airflow characteristics, illustrating sensitivity of aerodynamic performance to attack angle variations, particularly in low Reynolds number regimes relevant for small-scale applications [6].

Passive flow control studies on the NACA 0018 aerofoil using riblets showed that surface modifications can delay flow separation, reduce drag, and improve performance under low Reynolds number conditions [7]. RANS-based aerodynamic simulations of the NACA 0015 flapped aerofoil confirmed that CFD is capable of accurately predicting lift and drag characteristics, making it a reliable tool for aerofoil performance evaluation [8]. Numerical studies investigating both passive and active flow separation control over the NACA 0015 aerofoil underscored the significance of flow control strategies in enhancing lift and delaying stall [9]. Comparative analyses of turbulence models for the NACA 0018 aerofoil demonstrated that model selection critically influences CFD prediction accuracy, especially for complex flow phenomena such as separation and transition [10]. CFD modeling of the NACA 4412 aerofoil at varying angles of attack confirmed that its cambered profile improves lift-to-drag performance at low wind speeds, making it highly suitable for small- and medium-scale wind turbine applications [11]. The aerodynamic performance of the NACA 4415 aerofoil has been numerically analyzed, revealing its potential to enhance aircraft performance in applications requiring high lift and minimal drag [12].

Camber modifications significantly influence aerodynamic performance. Studies on variable camber-morphing airfoils showed that substantial camber deflections enhance lift but can increase drag, highlighting the need to optimize the lift–drag trade-off for high-lift aircraft and energy-efficient wind turbines [13]. Comparative analyses of NACA aerofoils using DeepCFD, conventional CFD, and 2D/2C PIV measurements confirmed strong agreement at low to moderate Reynolds numbers, validating CFD for aerodynamic analysis [14]. Simulations with COMSOL Multiphysics revealed that Reynolds number variations markedly affect lift and drag coefficients of wind turbine blades,

stressing its importance in high-speed performance [15]. Comparisons of CFD software for the NACA 2412 aerofoil indicated that solver choice and mesh strategy significantly affect lift, drag, and pressure predictions [16]. Numerical simulations of the NACA 6420 aerofoil with the transition RANS k-ε model highlighted the importance of turbulence modelling for accurate aerodynamic prediction under varied conditions [17]. These findings underline the role of camber optimization and advanced CFD modelling in enhancing aerodynamic efficiency across engineering applications.

CFD-based assessments of the NACA 0012 aerofoil have examined the effects of Reynolds number and angle of attack on lift and drag, demonstrating the strong influence of these parameters on overall aerodynamic behavior [18]. Experimental and numerical evaluations of NACA 4415 and NACA 0015 aerofoils over a wide range of angles of attack (50° to 200°) have provided valuable insights into their lift and drag characteristics and confirmed their applicability across diverse aerodynamic applications [19].

Various experiments have confirmed a direct relationship between Reynolds number and the aerodynamic performance of aerofoils such as NACA 4412, NACA 0012, and NACA 2415, showing that higher Reynolds numbers generally lead to increased lift and drag [20–22]. Additional studies have examined the interaction between blade pitch and wind velocity, providing recommendations for optimizing the use of specific aerofoils, such as NACA 0012 and NACA 4412, in various operating conditions [23]. Lift and drag comparison-based CFD studies further aid in selecting aerofoils that best suit particular flow conditions and energy requirements [24]. Experimental investigations on the NACA 4415 aerofoil focused on an improved version compared to the standard design, revealing that aerodynamic performance can be enhanced through targeted modifications [25]. Parametric simulations analyzing the effects of surface grooves demonstrated that appropriately designed surface changes can improve flow characteristics and overall aerofoil efficiency for specific applications [26]. Furthermore, studies on the influence of aerofoil type and rotor size on the efficiency of miniature wind turbines have provided important insights for optimizing small wind turbine designs, especially in off-grid power generation scenarios, by evaluating various aerofoil shapes in combination with rotor diameters [27].

A review of existing literature reveals that while several studies have analyzed NACA aerofoils such as 0012, 2412, 4412, and 4415 individually using CFD and experimental methods, comparative investigations focusing specifically on NACA 2412 and NACA 4415 under varying Reynolds numbers and wide ranges of angles of attack remain limited. Most prior works have concentrated either on optimization techniques, flow separation studies, or aerodynamic improvements through geometric modification or surface treatment, often restricted to low or moderate flow conditions. Furthermore, very few studies have systematically examined the combined influence of Reynolds number and angle of attack on both lift and drag performance using a computational method. This lack of a comprehensive comparative evaluation under identical simulation settings leaves a gap in understanding the relative aerodynamic efficiency and performance boundaries of these two widely used aerofoil profiles, especially in the context of small- and medium-scale wind energy and low-speed aerodynamic applications.

The present study bridges a significant research gap by conducting a comprehensive comparative CFD analysis of NACA 2412 and NACA 4415 aerofoils under varying flow conditions using ANSYS Fluent. While both aerofoils are extensively used in aircraft and wind turbine applications, limited studies have systematically examined their relative aerodynamic performance across different Reynolds numbers and angles of attack under identical conditions. This work uniquely integrates aerodynamic performance assessment by evaluating lift coefficient (CL), drag coefficient (CD), lift force, and drag force over a wide operational range—Reynolds numbers from 10,000 to 200,000 and angles of attack from 0° to 60°. A finely structured C-type mesh was employed to ensure accurate flow capture around the aerofoils. The novelty of this research lies in its comparative approach that

reveals how geometric differences influence aerodynamic efficiency, lift generation, and drag behavior across flow regimes. The results demonstrate that NACA 4415 provides superior lift performance at moderate AOAs, whereas NACA 2412 offers relatively stable aerodynamic characteristics, thereby providing design insights for selecting appropriate aerofoil profiles in wind turbine, UAV, and aerodynamic surface applications.

METHODOLOGY

The grounds of the methodology are the comprehensive CFD computations of the NACA 4415 and NACA 2412 profiles aerodynamic efficiency. This theory is adopted in the research in a methodical manner as the research plans to involve selecting aero foil, computational modeling, meshing, setting the simulation and analyzing the results. The most important actions are presented below:

Aerofoil Selection and Geometry Creation

- NACA 4415 and NACA 2412 aerofoils are chosen since their aerodynamic use are well distinguished.
- The NACA aerofoil generator tools, including NASA tool or AerofoilTools.com, provides the aerofoil coordinates.
- The geometry of the 2D aerofoil profiles defining the geometry is done using ANSYS.

Computational Domain and Meshing

- A rectangular computational domain is created to simulate airflow around the aerofoils, ensuring proper boundary conditions and minimizing flow interference.
- A structured/unstructured mesh is generated using ANSYS Meshing refining the grid near the aerofoil surface for better accuracy.
- The process of conducting a grid independence study involves making adjustments to the mesh and comparing the outcomes to guarantee the correctness of the solutions and numerical stability.

Governing Equations and CFD Solver Setup

- The RANS equations, which regulate fluid motion, are used in these computational fluid dynamics (CFD) simulations.
- A suitable turbulence model is selected for turbulence modeling, depending on accuracy and computational efficiency.
- Incompressible, steady-state airflow is assumed since the study focuses on subsonic aerodynamics.

Boundary Conditions and Flow Parameters

Velocity Inlet Boundary Condition

- A uniform free stream velocity (e.g., 5–30 m/s) is set at the inlet.
- Atmospheric pressure is used at the output as a boundary condition to enable unrestricted flow.
- A no-slip condition is used to simulate the effects of viscosity on an aerofoil's surface.
- The variations in lift and drag are analyzed by running the simulations at different angles of attack (AoA), which range from 0° to 60°.

Numerical Solution and Post-Processing

- The simulations are run in ANSYS using an iterative solver for pressure-velocity coupling.
- *Convergence criteria:* The solution is monitored until residuals drop below 10^{-5}, ensuring stability and accuracy.

Post-processing in ANSYS CFD-Post

- The coefficients for lift (C_L) and drag (C_D) are determined.

- Visualizations are made of pressure contours, turbulence effects, and velocity streamlines. One way to measure efficiency is by looking at the lift-to-drag ratio, or C_L/C_D.

Geometry Modeling and Flow Domain Creation

This study explores aerodynamic performance of two aerofoil profiles—NACA 4415 and NACA 2412—designed according to the conventional NACA four-digit series specifications. The coordinate data for each profile was obtained from the Airfoil Tools website and subsequently imported into ANSYS DesignModeler to create accurate two-dimensional aerofoil surfaces. For consistency in comparison, a chord length of 100 mm was used for both aerofoils. To analyze the external flow around the aerofoils, a C-type computational domain was created for each case. This domain consists of a semicircular leading-edge region with a radius of 1 meter and a rectangular trailing-edge extension also 1 meter in length-both dimensions being 10 times the chord length, providing sufficient space for flow development and minimizing domain boundaries' impact on the outcomes. To accurately characterize the fluid area around the body, the aerofoil surface was removed from the flow domain. After that, designated selections were allocated to various boundary areas, including the walls, the inlet, the outflow, and the aerofoil surface, to facilitate the setup of boundary conditions during the CFD simulations. The geometries of the NACA 2412 and NACA 4415 aerofoils along with their respective flow domains are shown in Figure 1.

Mesh Generation

The 2D model of each aerofoil immersed in structured meshing techniques were then used to discretize a fluid domain. The mesh refinement surrounding the aerofoil received particular attention. surfaces by applying edge sizing, face meshing, and biasing. This created a fine mesh near the aerofoil boundary, which is critical for accurately capturing boundary layer behavior and flow separation. Inflation layers were also added near the walls to improve near-wall resolution. The resulting mesh structures for considered aerofoils are shown in Figure 2.

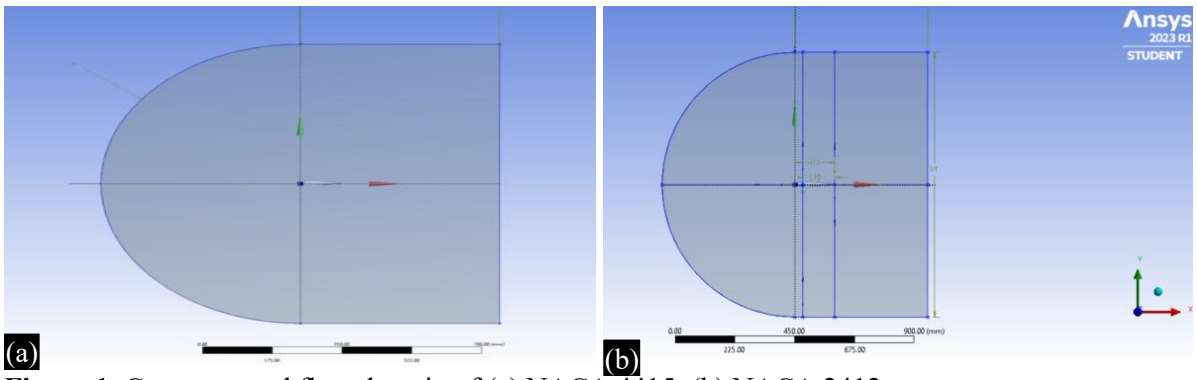

Figure 1. Geometry and flow domain of (a) NACA 4415; (b) NACA 2412.

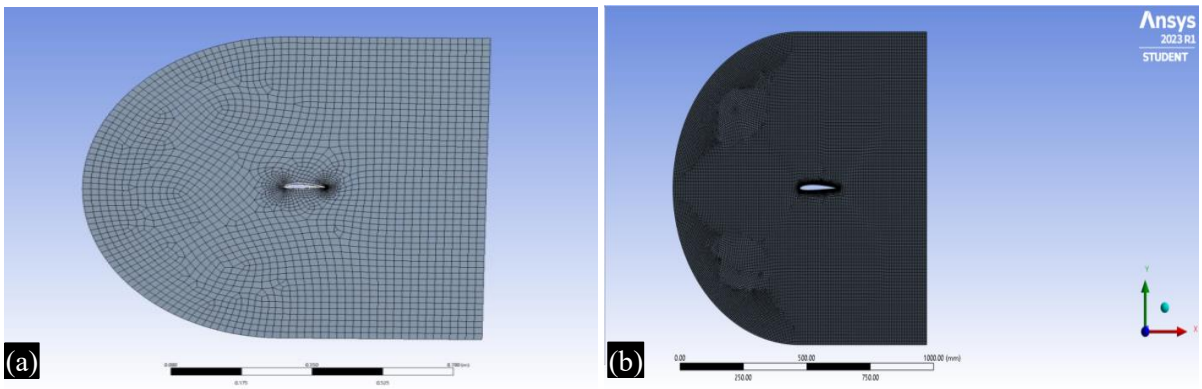

Figure 2. Mesh structure of (a) NACA4415; (b) NACA2412

COMPUTATIONAL ANALYSIS

The simulated aerodynamic performance is the main emphasis of this work evaluation of two widely used aerofoil profiles-NACA 4415 and NACA 2412-utilizing ANSYS Fluent. The objective is to assess the variation in the relationship between lift and drag forces and angle of attack, Reynolds number (Re), and inlet velocity, with specific application to horizontal-axis blades of wind turbines with low to moderate Reynolds numbers. A two-dimensional, steady-state, incompressible turbulent flow simulation was carried out using the k-ε turbulence model in ANSYS Fluent. The simulation domain was created around each aerofoil with a improved boundary layer mesh to precisely depict flow behavior close to walls. Each aerofoil was analyzed at five different angles of attack (AoA): 0°, 15°, 30°, 45°, and 60°, covering pre-stall, stall, and post-stall regimes. The simulations were run with Reynolds numbers between 10,000, 50,000, 100,000, 150,000, and 200,000, with corresponding inlet velocities ranging from 1.47 m/s to 29.55 m/s.

The NACA 4415 aerofoil's lift and drag forces demonstrated a steady rise in lift with angle of attack up to 30°, beyond which a stall-like behavior began to emerge—evidenced by a reduction or saturation in lift and a sharp rise in drag. At Re = 200,000 and AoA = 30°, the lift peaked at 777.25 N, while drag reached 209.20 N, highlighting the aerofoil's strong performance before flow separation became dominant. Similarly, the NACA 2412 aerofoil was analyzed under the same set of conditions.

The computational results indicated a relatively lower lift generation at less aggressive angles than the NACA 4415, but with greater stable drag behavior across the tested range. At Re = 200, 000 and AoA = 45°, the lift force magnitude reached a maximum of 86.69 N, and the drag force became 82.10 N, and the flow stall occurred. The drag and lift analysis of both NACA 4415 and NACA 2412 aerofoil explains the results obtained in all the test conditions as summarized in Table 1. The findings can also be shown graphically in Figures 3–6 showing pressure fields and confined areas of flow separation.

Table 1. Drag and lift forces – NACA 4415 & NACA 2412 aerofoil

S.N.	Reynolds number (Re)	Velocity in (m/s)	AOA (angles of attack) in degree	NACA 4415		NACA 2412	
				Drag force (N)	*Lift force (N)*	*Drag force (N)*	*Lift force (N)*
1.	10000	1.4770	0°	0.1892	1.7477	0.005714	0.000372
			15°	0.2714	1.4194	0.037992	0.012186
			30°	0.4544	1.9552	0.10863	0.20973
			45°	0.2367	1.4150	0.21054	0.21226
			60°	0.5430	1.3563	0.3634	0.20173
2.	50000	7.3877	0°	0.5750	14.4391	0.11688	0.63149
			15°	4.1009	36.1056	0.87302	3.2847
			30°	12.5322	48.5261	2.6941	5.3148
			45°	8.2808	37.4073	5.1751	5.3900
			60°	2.3359	35.1387	8.3423	5.0968
3.	100000	14.7755	0°	2.0366	57.9351	0.4138	3.8314
			15°	16.7303	145.3902	3.4068	13.437
			30°	32.3522	195.9259	10.792	21.311
			45°	14.8984	94.2276	20.648	21.630
			60°	10.3098	141.2990	33.270	20.040
4.	150000	22.1632	0°	4.3082	130.7019	8.855	0.86084
			15°	38.0288	329.0228	30.405	7.5661
			30°	117.8332	437.9432	24.405	43.633
			45°	61.0680	315.9920	46.206	48.702
			60°	25.2634	327.6098	42.949	25.595

5.	200000	29.5510	0º	7.3479	232.8	1.4622	15.956
			15º	68.0480	586.22	13.306	54.309
			30º	209.2039	777.25	43.212	77.343
			45º	110.8556	569.48	82.106	86.687
			60º	41.8434	577.92	76.084	45.391

RESULTS AND DISCUSSION

Analysis of fluid flow in NACA 2412 and NACA 4415 aerofoils the aerodynamic properties of these two were assessed and compared using ANSYS Fluent at different flow conditions. Parametric studies are conducted with Reynolds numbers of 10,000 to 200,000, and angle of attacks (AoA) between 0º-60º that characterize the level of operation in small-scale wind turbine optimization.

Lift and Drag Trends

The two aerofoils have the same patterns of aerodynamics. The increasing angle of attacks and Reynolds numbers caused the steady increment in the lift and drag forces within some specific angle of attack or limit of attack angles. Beyond this, especially beyond 30° AoA, signs of flow separation and stall were observed, particularly for the NACA 2412 aerofoil.

- At Re = 200,000 and an angle of attack of 30°, the NACA 4415 aerofoil achieved apeak lift force of 777.25 N and a drag force of 209.20 N.
- For NACA 2412, a maximum lift force of 86.69 N and drag force of 82.11 N were observed at AoA = 45° and Re = 200,000.
- NACA 4415's greater camber contributes to superior lift generation, whereas NACA 2412 demonstrates more balanced lift-drag behavior across a wider AoA range.

Pressure and Velocity Contours

The pressure and velocity distribution contour plots from the computational fluid dynamics (CFD) model revealed:

- A distinct stagnation point at the leading edge.
- Zones of high velocity over the top surface with lower pressure, as expected by Bernoulli's principle.
- Aerodynamic lift is a result of the difference in pressure that acts on the aerofoil's top and lower surfaces.
- At higher AoA, flow separation is evident, especially in the NACA 2412 results, causing a drop in lift and surge in drag.

Using ANSYS, the NACA 4415 airfoil was analyzed, and Figures 3 and 4 presents sample results for a Reynolds number of 200,000 and a velocity of 29.55 m/s. Figure 3 (a) and Figure 4 (a) display the airfoil's pressure and velocity contours at a 0 degree angle of attack, respectively.

ANSYS was used to analyze the NACA 2412 airfoil, and Figures 5 and 6 presents typical results for Re = 200,000 at a velocity of 29.55 m/s. Figure 5 (a) and Figure 6 (a) specifically show the pressure and velocity contours, respectively, for the airfoil at a 0° angle of attack.

Lift and Drag Coefficient Behavior

The lift coefficient (C_L) and drag coefficient (C_D) for both aerofoils followed similar patterns. With increasing AoA and Reynolds number:

- C_L increased steadily until stall onset (approximately 30°–45°).
- C_D increased more rapidly at higher angles due to turbulent separation.
- NACA 4415 showed optimum aerodynamic performance at 30° AoA, while NACA 2412 peaked around 45° AoA.

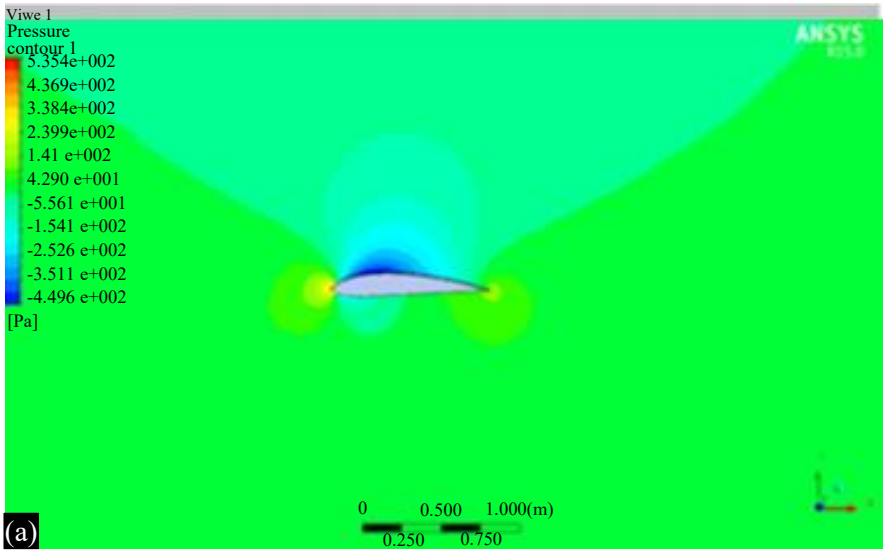

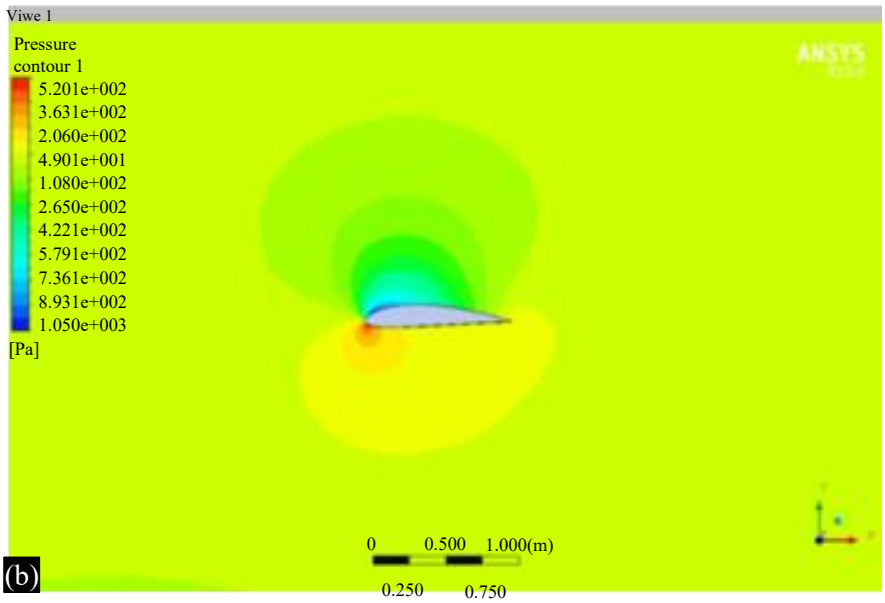

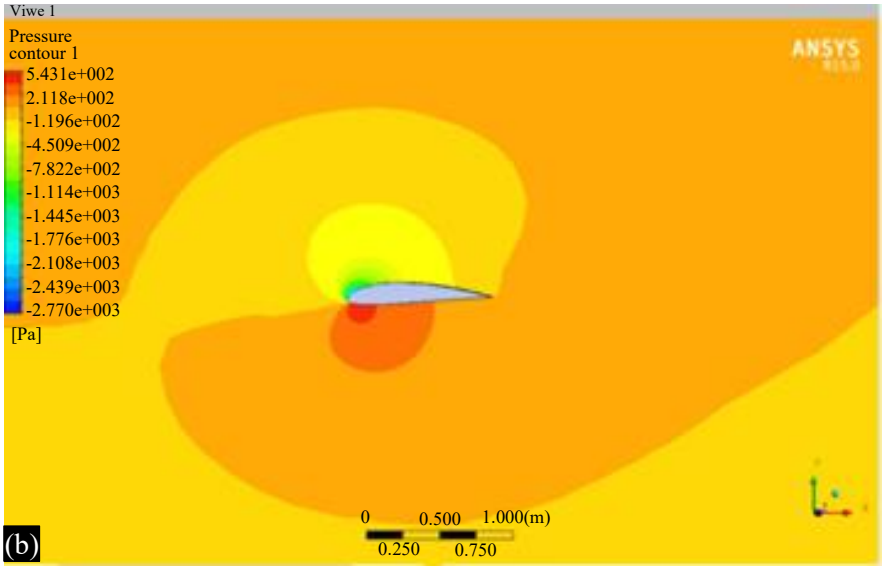

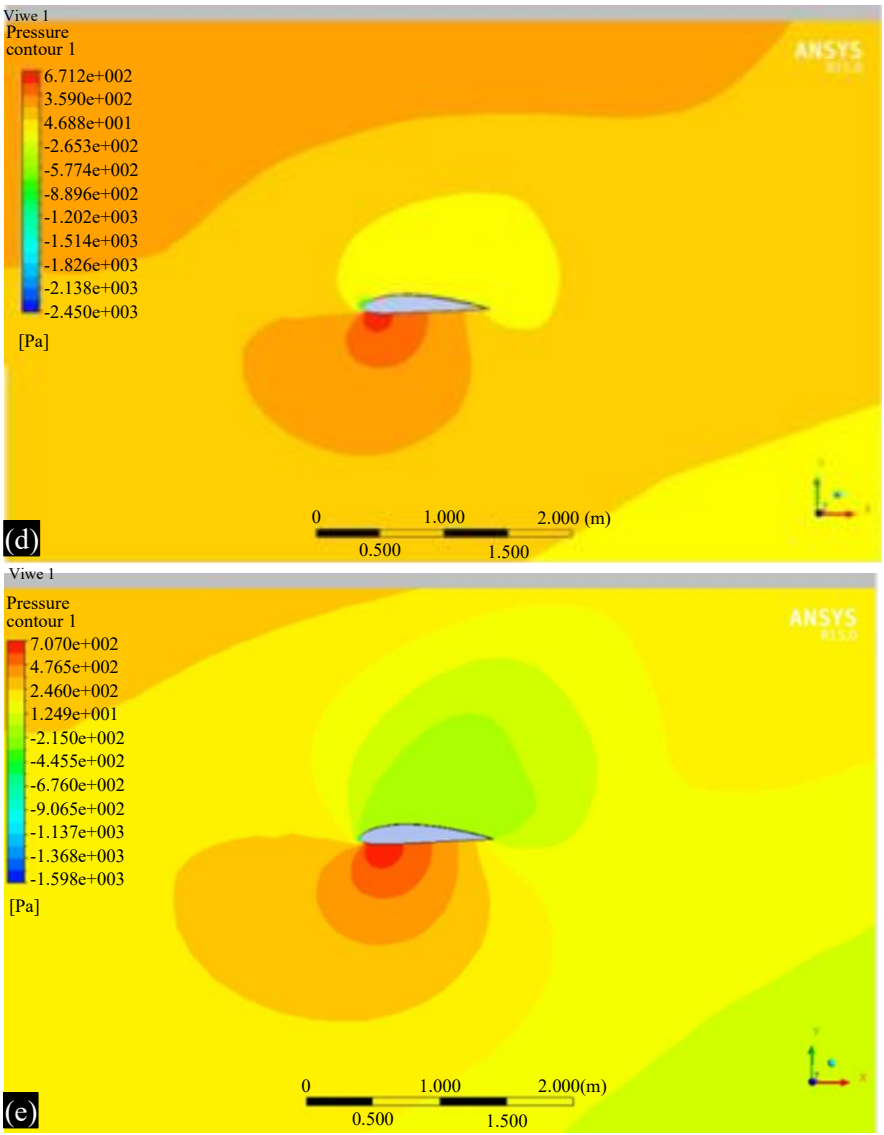

Figure 3. Pressure contours for NACA 4415 at angles of attack (AOA) of 0°, 15°, 30°, 45°, and 60° - Subfigures (a) to (e) respectively.

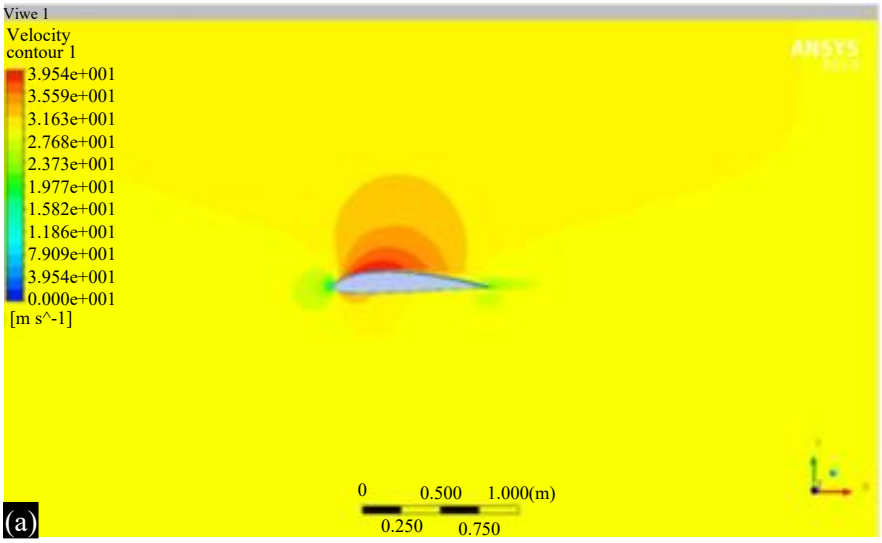

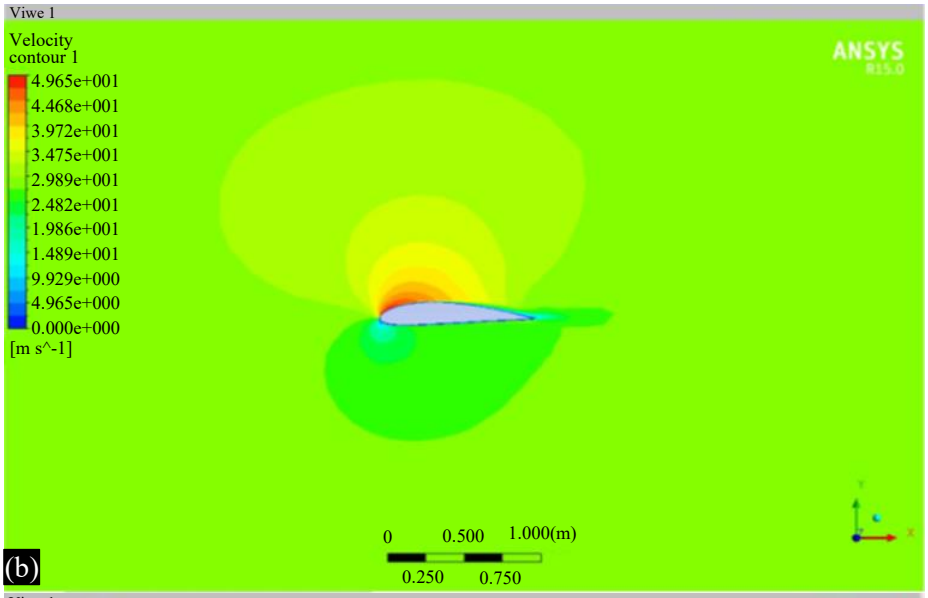

(b)

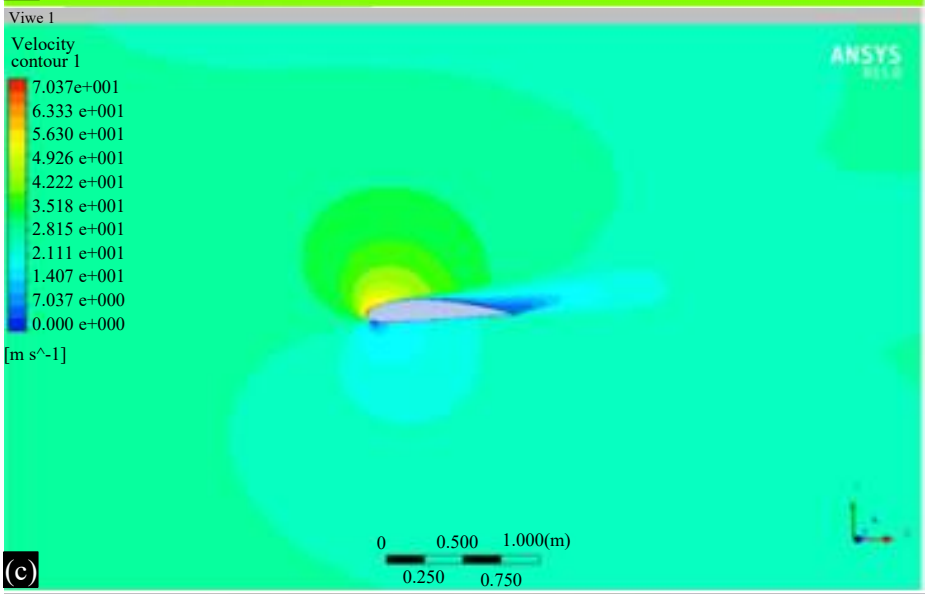

(c)

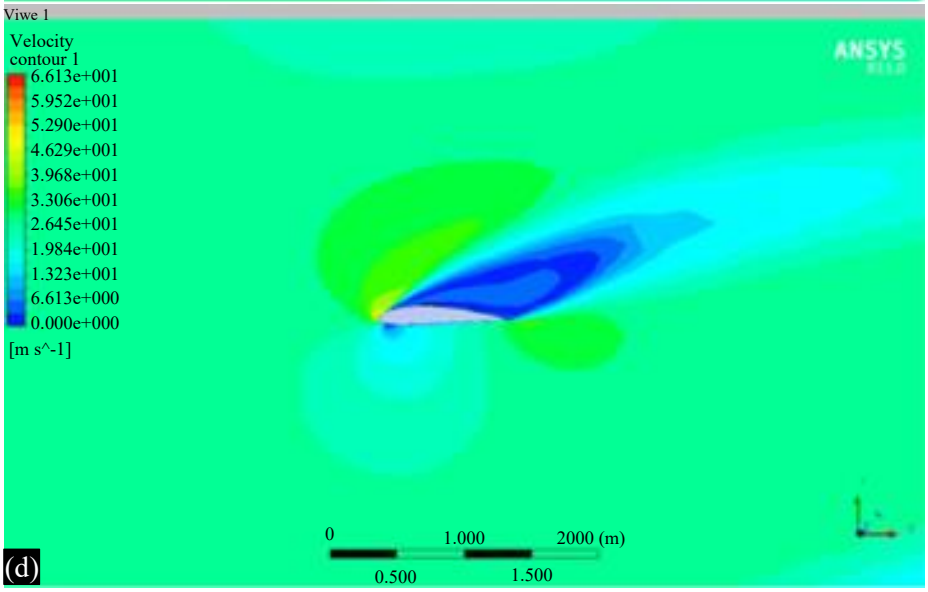

(d)

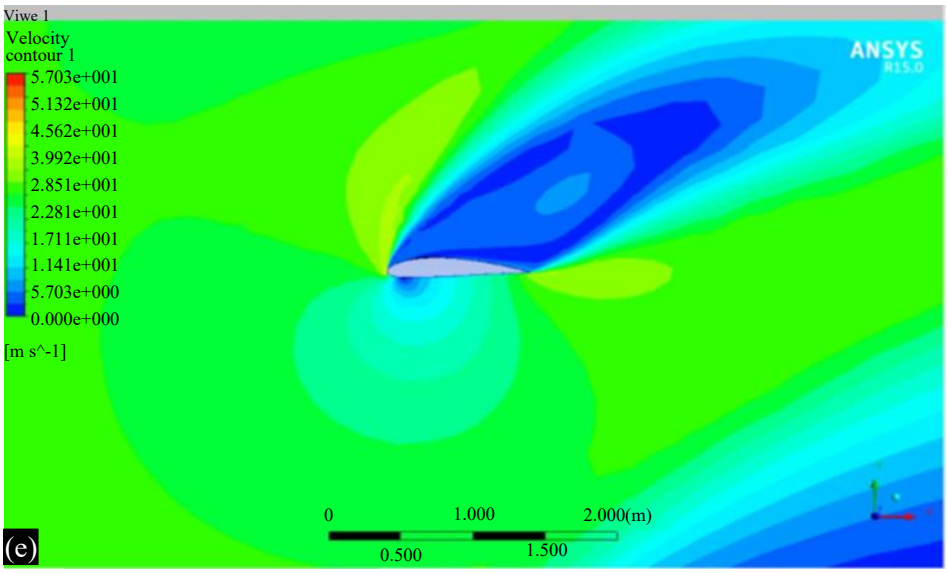

Figure 4. Velocity contours for NACA 4415 at angles of attack (AOA) of 0°, 15°, 30°, 45°, and 60° - Subfigures (a) to (e) respectively.

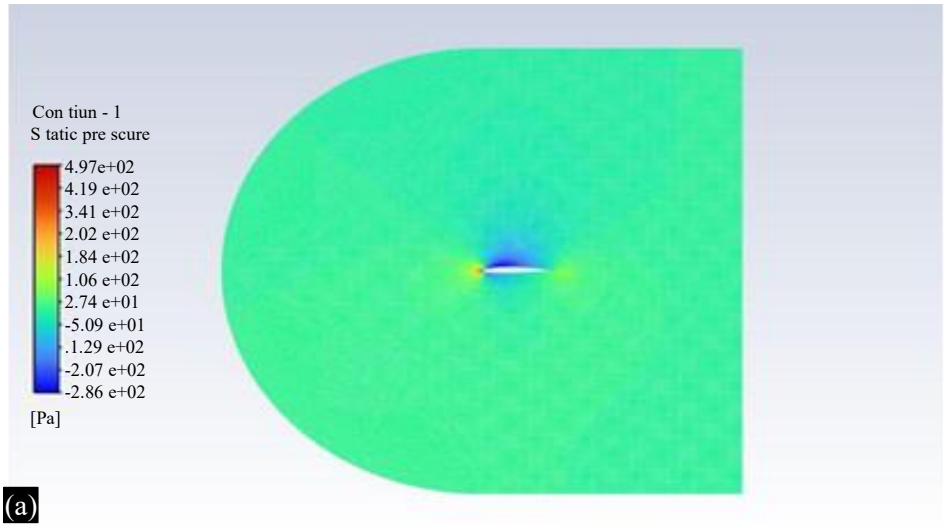

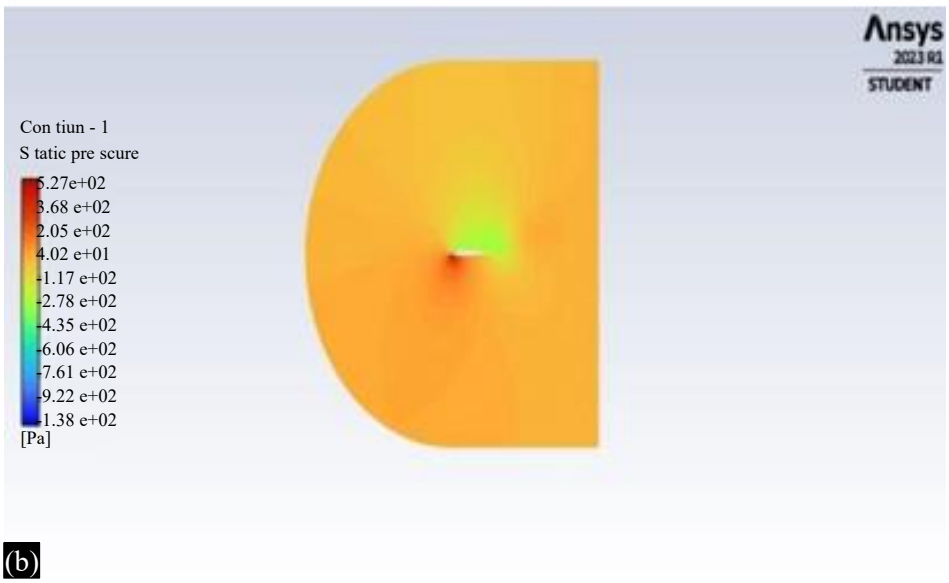

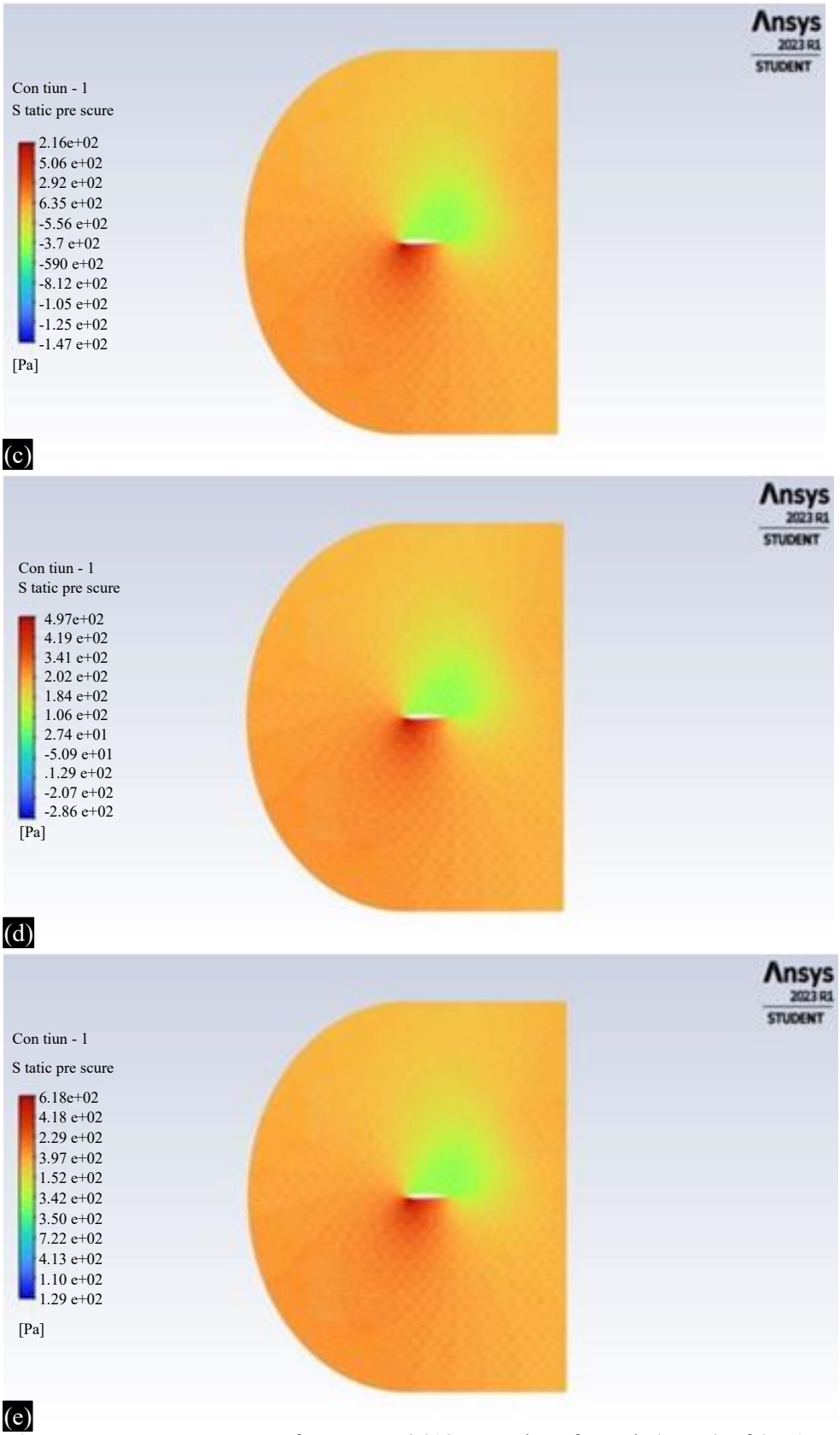

Figure 5. Pressure contours for NACA 2412 at angles of attack (AOA) of 0°, 15°, 30°, 45°, and 60° - Subfigures (a) to (e) respectively

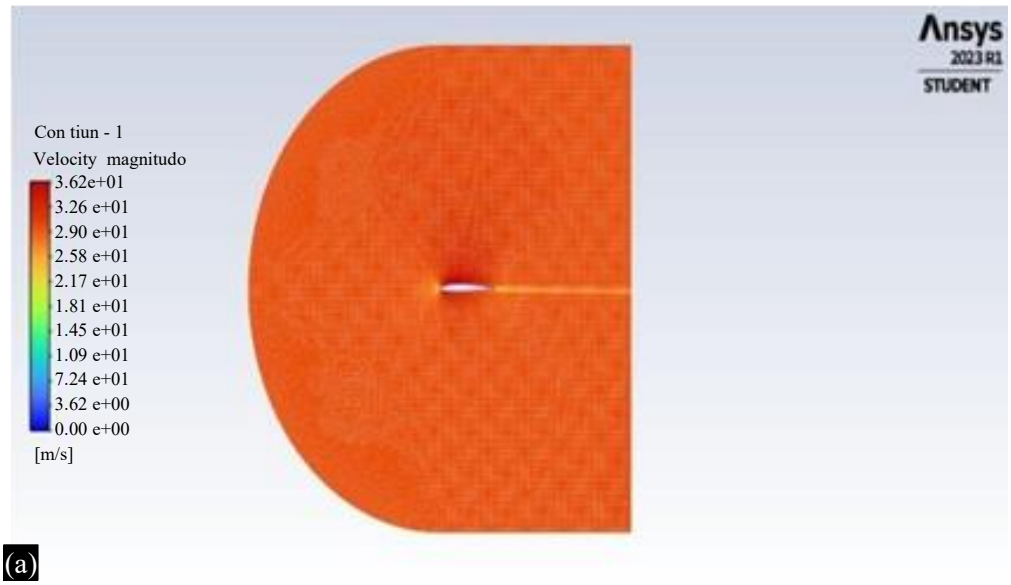

(a)

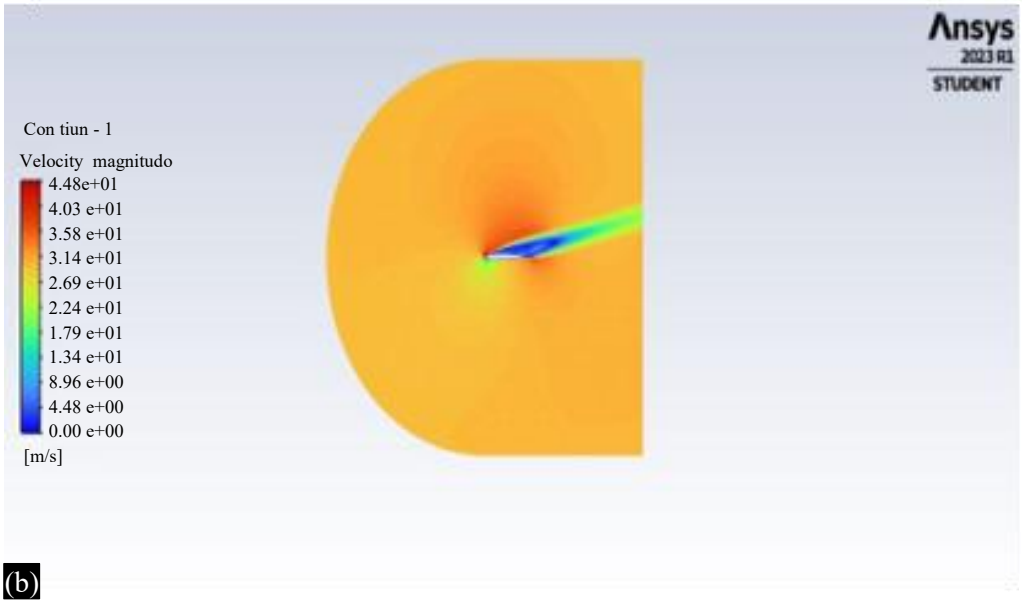

(b)

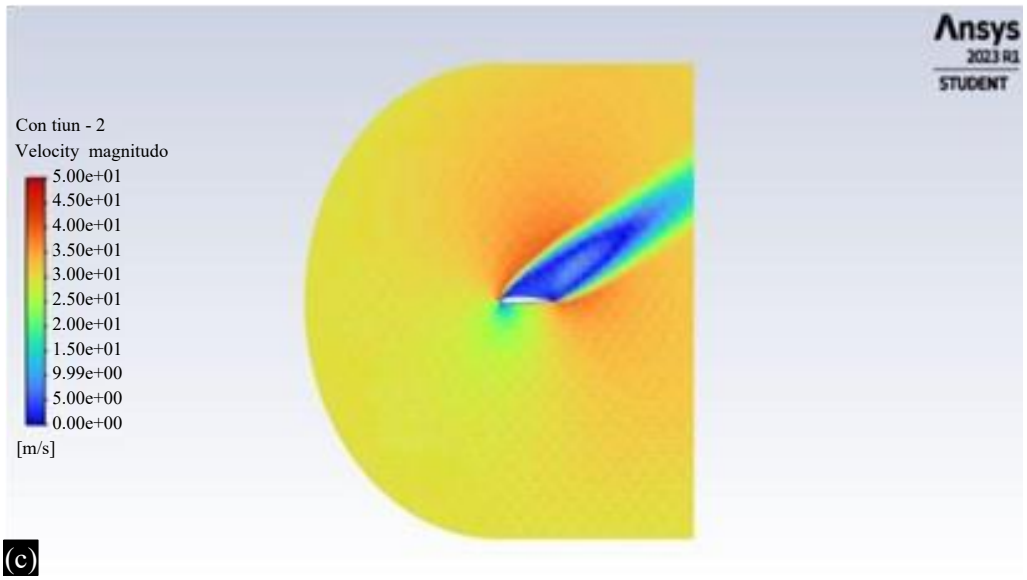

(c)

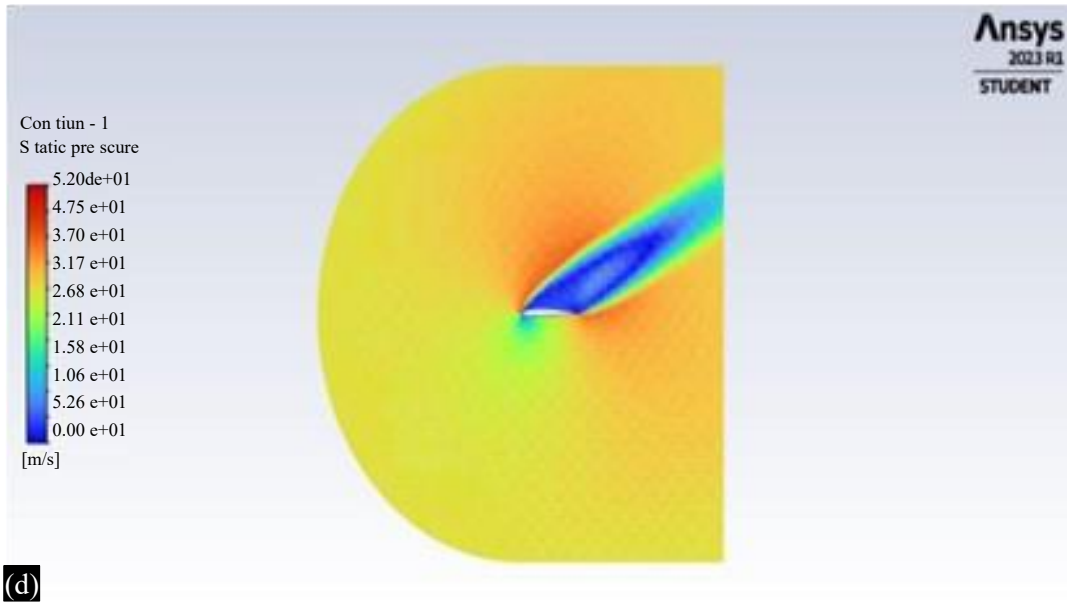

(d)

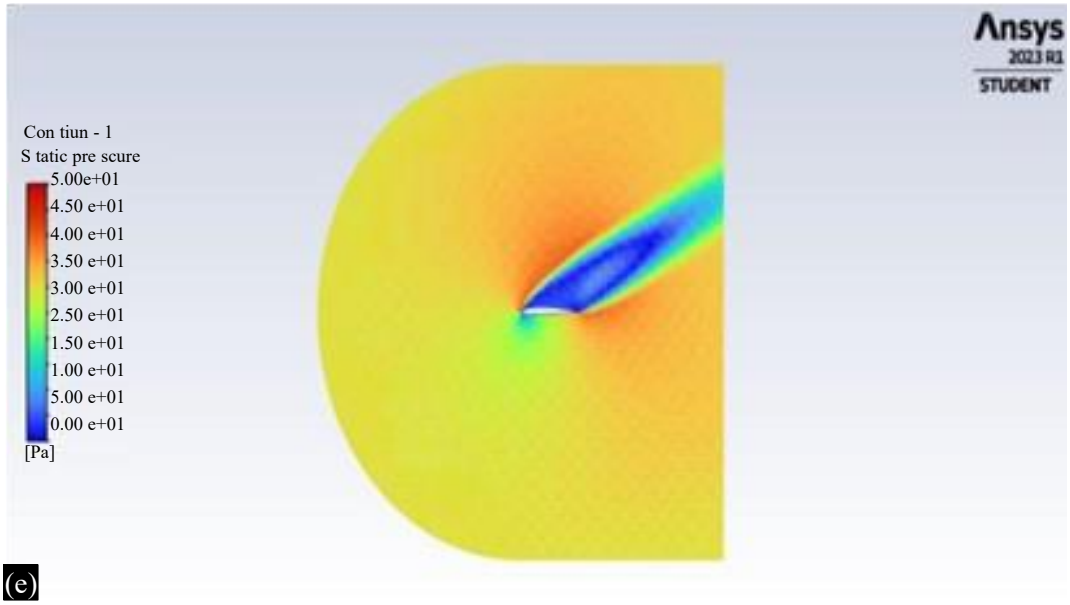

(e)

Figure 6. Velocity contours for NACA 2412 at angles of attack (AOA) of 0°, 15°, 30°, 45°, and 60° - Subfigures (a) to (e) respectively.

Table 2. Comparative performance summary – NACA 4415 & NACA 2412 aerofoil.

Parameter	NACA 2412 (ANSYS)	NACA 4415 (ANSYS)
Max Lift Force (N)	86.69 at 45°, Re 200,000	777.25 at 30°, Re 200,000
Max Drag Force (N)	82.11 at 45°, Re 200,000	209.20 at 30°, Re 200,000
Best AoA for Max Lift	45°	30°
Reynolds Number Range	10,000 – 200,000	10,000 – 200,000

Comparative Performance Summary

The comparative summary reveals that NACA 4415 significantly outperforms NACA 2412 in terms of maximum lift, especially at lower angles of attack as illustrated in Table 2. However, NACA 2412 demonstrates a more gradual and stable aerodynamic response, making it appropriate for uses where a smoother lift is needed-to-drag characteristics are preferred.

Discussion

From the detailed CFD simulation results:

- NACA 4415 continues to give superior performance to NACA 2412 in lifting maximum force which is favourable over energy extraction in wind turbine blades.
- NACA 2412 shows a smoother aerodynamic performance with less drag penalty at the higher AoAs and it is desirable to use in low-Reynolds-number UAV or in general aviation.
- Both aerofoils perform stall properties after 30^0-45^0AoA of their angle of attack, which also highlights the necessity to keep the optimal degrees of their functionality.

Comparison of C_L, C_D, and C_L/C_D between the Two Aerofoils

Three important coefficients are the primary features of the aerodynamic efficiency of an aerofoil: Drag Coefficient (C_D), Lift Coefficient (C_L), and their ratio (C_L/C_D), which combined together define the capability of aerofoil to create lift as compared to the aerodynamic resistance it comes across. On this part, comparative analysis of NACA 2412 and NACA 4415 is done according to these performance parameters against different Reynolds numbers (Re) and angles of attack (AoA).

Lift Coefficient (C_L) Comparison

In all the Reynolds tested, the NACA 4415 was found to have higher value than NACA 2412 in all cases. Higher camber in NACA 4415 allows greater pressure crack across the top and bottom sides, resulting in greater production of lift. Peak C_L values were observed at 30° AoA for NACA 4415, whereas NACA 2412 peaked at 45° AoA. At Re = 200,000, NACA 4415 showed a C^L of approximately 2.91, while NACA 2412 reached around 0.94, highlighting the superior lift performance of the 4415 aerofoil.

Drag Coefficient (C_D) Comparison

Although NACA 4415 was found to have more lift in comparison, the higher lift was accompanied by greater drag coefficients, especially in exceeding 30^oAoA. The higher camber and curvature of the surface cause early separation at higher AoA which causes the form drag to be high. Conversely, NACA 2412 achieved lower C_D at a wider range of AoA especially at the low Reynolds number condition, indicating its relatively smoother flow motion and late stall.

Lift-to-Drag Ratio (C_L/C_D) Comparison

The C_L/C_D ratio serves as a direct measure of aerodynamic efficiency. Despite the higher lift of NACA 4415, its increased drag reduces its C_L/C_D ratio at high AoAs as shown in Table 3. NACA 2412 demonstrated a more favorable C_L/C_D ratio at lower and moderate AoAs, particularly up to 30°, indicating better efficiency in cruising or low-angle flight conditions. However, NACA 4415 outperformed in terms of C_L/C_D at 30° AoA under higher Reynolds numbers, making it optimal for applications demanding high lift generation, like small-scale wind turbines.

Table 3. Summary of observations.

Parameter	NACA 2412	NACA 4415
Max C_L	~0.94 at 45°, Re 200,000	~2.91 at 30°, Re 200,000
Max C_D	Lower overall, peaks at higher AoA	Higher overall, increases after 30° AoA
Optimal C_L/C_D	At lower AoA (15°–30°)	At ~30° under high Re
Efficiency (C_L/C_D)	More stable across AoA	High lift but lower efficiency at high AoA

The review states that although NACA 2412 improves aerodynamic performance through varying conditions, NACA 4415 gains more lift and therefore is a good selection when high thrust is the main concern like during wind turbine usage or a short-takeoff.

CONCLUSIONS

This study consisted of a Computational Fluid Dynamics (CFD) simulation of the two popular aerofoils namely NACA 2412 and NACA 4415 aerofoils with the object to determine their aerodynamics performance with respect to lift and drag forces at different flow rates. Simulations were carried out using ANSYS Fluent, covering Re from 10,000 to 200,000 and AOA ranging from 0° to 60°. The results provide valuable information towards the aerodynamics of such aerofoil surfaces especially in wind energy application, in unmanned aerial vehicles (UAVs) and in low-speed aircraft.

Some important observations in this study are as follows:

1. The existence of more camber of NACA 4415 led to consistently greater lift forces being generated with the maximum lift of 777.25 N generated by Re = 200,000 and 30^0AoA which confirms that it could be implemented in high-lift devices such as wind power turbine blades.
2. NACA 2412 had greater stabilized aerodynamic character under a broader angle and a maximum lift of 86.69 N was obtained at 45^0AoA at Re = 200,000. Its performance balance indicates its suitability in various opinions, which raise the need of lift and the aerodynamic stability.
3. The two aerofoils showed their propensity to increase the lift and the drag as the Reynolds numbers and the AoAs increased, with NACA 4415 showing more pronounced increase in the lift and the drag, especially at lower AoAs.
4. NACA 4415 and NACA 2412 were seen to experience the best values of lifting at 30^0 and 45^0 respectively as the experiment saw each aerofoil reach their individual peak results.
5. A percentage growth analysis pointed out that the greatest gains in both lift and drag aerodynamic occurred at lower Reynolds numbers especially during Re = 10,000-50,000 with NACA 2412 had rapid initial growth in its performance sense.

Finally, the comparison of NACA 2412 and NACA 4415 should be based on the purpose it is intended to use:

- NACA 4415 is perfect in situations that demand high lift e.g. in wind energy generation.
- NACA 2412 has smoother lift-to-drag transition, and is more suited to smooth, moderate-lift conditions like general aviation and UAVs.

Future endeavor can be made to generalize this analysis with the turbulence transition models, 3D effects and experimental validation in wind tunnel to add more correctness and applicability of the result.

REFERENCES

1. Kharulaman L, Aabid A, Mehaboobali FA, Khan SA. Research onFlows for NACA 2412 Airfoil using computational fluid dynamics method. Int. J. Eng. Adv. Technol. 2019;9(1):5450–6.
2. Sandeep D, Ravitej YP, Khot S, Ravikumar R, Abhinandan, Kumar N, Karthik SB, Veerachari. CFD simulation of transonic turbulent flow past NACA 0012 aerofoil. InAIP Conference Proceedings 2021 Feb 16 (Vol. 2316, No. 1, p. 020013). AIP Publishing LLC.
3. Srivastava S, Aditya CV. Analysis of NACA 2412 Airfoil for UAV Based on High-Lift Devices. International Journal of Engineering Applied Sciences and Technology. 2016;1(6):13–6.
4. Saeed S, Abdulla S, Shaheen S, Saeed A, Thaher A, Khan SH. Optimizing NACA airfoils for sustainable medical delivery UAVs: Aerodynamic analysis. Progress in Engineering Science. 2025 Jun 1;2(2):100067.
5. Badu P, Panjiyar R, Guragain K, Yadav P. CFD Analysis of Rear Spoiler Effects on Vehicles Aerodynamic Performance. OODBODHAN. 2024 Dec 31;7:16–22.
6. Chen H, Mei H, Yi G. Exploring the Influence of NACA0018 Airfoil Attack Angle on the Airflow Characteristics Based on CFD. In: Proceedings of the 1st International Conference on

Modern Logistics and Supply Chain Management (MLSCM 2024), 2024 Oct 16–18; Bangkok, Thailand. SciTePress; 2025. p. 497–504.
7. Güler E, Durhasan T, Karasu İ, Akbıyık H. Passive flow control around NACA 0018 airfoil using riblet at low reynolds number. Journal of the Institute of Science and Technology. 2021 Sep;11(3):2208–17.
8. Obeid S, Jha R, Ahmadi G. RANS simulations of aerodynamic performance of NACA 0015 flapped airfoil. Fluids. 2017 Jan 5;2(1):2.
9. Larbi M, Yahiaoui T, Belkadi M, Adjlout L, Ladjedel O, Šikula O. Numerical study of passive and active flow separation behavior over NACA 0015 airfoil. International Journal of Fluid Machinery and Systems. 2020;13(2):327–35.
10. Khan SA, Bashir M, Baig MA, Ali FA. Comparing the effect of different turbulence models on the CFD predictions of NACA0018 airfoil aerodynamics. CFD letters. 2020;12(3):1–0.
11. Mukhti MA, Didane DH, Ogab M, Manshoor B. Computational fluid dynamic simulation study on NACA 4412 airfoil with various angle of attacks. Journal of Design for Sustainable and Environment. 2021;3(1).
12. Kashid D, Parkhe A, Wangikar S, Jadhav SV. Analysis of Drag and Lift Forces with Different Angle of Attacks on Airfoil used Analysis of Drag and Lift Forces with Different Angle of Attacks on Airfoil used in Aircraft Wings. NOVYI MIR Res. J. 2020;5(6).
13. Marciniuk M, Piskur P, Kiszkowiak Ł, Malicki Ł, Sibilski K, Strzelecka K, Kachel S, Kitowski Z. Aerodynamic analysis of variable camber-morphing airfoils with substantial camber deflections. Energies. 2024 Apr 9;17(8):1801.
14. Berger M, Raffeiner P, Senfter T, Pillei M. A comparison between 2D DeepCFD, 2D CFD simulations and 2D/2C PIV measurements of NACA 0012 and NACA 6412 airfoils. Engineering Science and Technology, an International Journal. 2024 Sep 1;57:101794.
15. Abood YA, Abdulrazzaq OA, Habib GS, Haseeb ZM. Determination of the Optimum Aerodynamic Parameters in the Design of Wind Turbine Using COMSOL Multiphysics Software. Iraqi Journal of Industrial Research. 2022 Oct 20;9(2):77–85.
16. Hetyei C, Molnár I, Szlivka F. Comparing different CFD software with NACA 2412 airfoil. Progress in Agricultural Engineering Sciences. 2020 Dec 12;16(1):25–40.
17. Alabi OO, Salisu SA, Aforolagba-Balogun OT, Ladigbolu TA, Fasina AO, Bala A. Numerical simulation of Airflow Properties of the NACA 6420 Airfoil Using the Transition RANS k-ε Model. Al-Bahir Journal for Engineering and Pure Sciences. 2025;6(1):8.
18. Patil BS, Thakare HR. Computational fluid dynamics analysis of wind turbine blade at various angles of attack and different Reynolds number. Procedia Engineering. 2015 Jan 1;127:1363–9.
19. Haque MN, Ali M, Ara I. Experimental investigation on the performance of NACA 4412 aerofoil with curved leading edge planform. Procedia Engineering. 2015 Jan 1;105:232-40.
20. Shaha SN, Pachapuri MS. NACA 2415-Finding Lift Coefficient Using CFD, Theoretical and Javafoil. International Journal of Research in Engineering and Technology04. 2015;7:444-9.
21. Rubel RI, Uddin MK, Islam MZ, Rokunuzzaman M. Comparison of Aerodynamics Characteristics of NACA 0015 & NACA 4415.
22. Yılmaz M, Köten H, Çetinkaya E, Coşar Z. A comparative CFD analysis of NACA0012 and NACA4412 airfoils. Journal of Energy Systems. 2018 Dec;2(4):145–59.
23. Avvad M, Vishwanath KC, Kaladgi AR, Muneer R, Kareemullah M, Navaneeth IM. Performance analysis of aerofoil blades at different pitch angles and wind speeds. Materials Today: Proceedings. 2021 Jan 1;47:6249–56.
24. Kulshreshtha A, Gupta SK, Singhal P. FEM/CFD analysis of wings at different angle of attack. Materials Today: Proceedings. 2020 Jan 1;26:1638–43.
25. Huda S, Rusianto T. Prediction of aerodynamics coefficients of modified NACA 4415 airfoil using computational fluid dynamics. InE3S Web of Conferences 2020 (Vol. 202, p. 11002). EDP Sciences.

26. Liu Y, Li P, He W, Jiang K. Numerical study of the effect of surface grooves on the aerodynamic performance of a NACA 4415 airfoil for small wind turbines. Journal of Wind Engineering and Industrial Aerodynamics. 2020 Nov 1;206:104263.
27. Yossri W, Ayed SB, Abdelkefi A. Airfoil type and blade size effects on the aerodynamic performance of small-scale wind turbines: Computational fluid dynamics investigation. Energy. 2021 Aug 15;229:120739.

